Editors' Suggestion

Emergence of a Fluctuating Ground State in Y-Kapellasite under Pressure

Dipranjan Chatterjee,[1,2,*] Petr Doležal,[3,4] Federico Abbruciati,[5] Tobias Biesner,[6] Katharina M. Zoch,[7] Rustem Khasanov,[8] Shams Sohel Islam,[8] Guratinder Kaur,[9] Seulki Roh,[6] Francesco Capitani,[10] Joao Elias F. S. Rodrigues,[5] Gaston Garbarino,[5] Cornelius Krellner,[7] Philippe Mendels,[1] Edwin Kermarrec,[1] Martin Dressel,[6] Björn Wehinger,[5] Andrej Pustogow,[4] Fabrice Bert,[1] and Pascal Puphal[9,6,†]

[1]*Université Paris-Saclay, CNRS, Laboratoire de Physique des Solides, 91405 Orsay, France*
[2]*Clarendon Laboratory, Department of Physics, University of Oxford, Parks Road, Oxford OX1 3PU, United Kingdom*
[3]*Department of Condensed Matter Physics, Faculty of Mathematics and Physics, Charles University, Ke Karlovu 5, 121 16 Prague 2, Czech Republic*
[4]*Institute of Solid State Physics, TU Wien, 1040 Vienna, Austria*
[5]*European Synchrotron Radiation Facility, 71 Avenue des Martyrs, F-38043 Grenoble, France*
[6]*1. Physikalisches Institut, Universität Stuttgart, Pfaffenwaldring 57, 70569 Stuttgart, Germany*
[7]*Physikalisches Institut, Goethe-Universität Frankfurt, Frankfurt am Main, Germany*
[8]*Laboratory for Muon-Spin Spectroscopy, Paul Scherrer Institut, 5232 Villigen, Switzerland*
[9]*Max-Planck-Institute for Solid State Research, Heisenbergstraße 1, 70569 Stuttgart, Germany*
[10]*Synchrotron SOLEIL, L'Orme des Merisiers Départementale 128, 91192 Saint-Aubin, France*

(Received 15 September 2025; revised 26 January 2026; accepted 2 March 2026; published 30 March 2026)

Y-kapellasite [$Y_3Cu_9(OH)_{19}Cl_8$], which hosts an original anisotropic kagome sublattice, is a promising candidate for studying elusive and complex correlated physics. It exhibits a theoretically predicted in-plane $(1/3, 1/3)$ magnetic order [Hering *et al.*, npj Comput. Mater. **8**, 1 (2022)], but its magnetic interaction values place it close to a phase boundary to a spin liquid state [Chatterjee *et al.*, Phys. Rev. B **107**, 125156 (2023)]. Our μSR measurements under hydrostatic pressure demonstrate the complete suppression of static magnetism in favor of a fully dynamical ground state at 2.3 GPa. Complementary high-pressure x-ray and optical phonon measurements reveal a gradual reduction of the kagome anisotropy, enhancing magnetic frustration without structural transitions. Our results establish Y-kapellasite as a rare clean kagome model in which long-range order is suppressed by pressure-tuned frustration, the first fingerprint for the realization of a quantum spin liquid without strong disorder.

DOI: 10.1103/3pmg-b78n

Geometric frustration is a key ingredient to prevent conventional magnetic ordering [1] and, in combination with enhanced fluctuations in low dimensional quantum magnets, to stabilize the long sought spin liquid ground states, which offer a platform for exploring long-range quantum entanglement and fractionalized excitations [2,3]. The search for quantum spin liquids (QSLs) in two-dimensional frustrated magnets has spurred extensive experimental efforts across a variety of geometries. Former work examined triangular systems such as κ-$(BEDT\text{-}TTF)_2Cu_2(CN)_3$ [4] or $YbMgGaO_4$ [5,6], and corner-sharing triangular kagome antiferromagnets including $ZnCu_3(OH)_6Cl_2$ [7,8], $ZnCu_3(OH)_6FBr$ [9], and $ZnCu_3(OH)_6FCl$ [10], all of which display experimental signatures of QSL behavior. In these systems, however, the determination of the true ground state is complicated by chemical or structural disorder, which can mimic the features expected for a perfectly frustrated QSL [11–18].

Among kagome antiferromagnets, herbertsmithite $ZnCu_3(OH)_6Cl_2$ stands as the archetypal example, extensively studied with a range of experimental probes [9,19–22]. Inspired by Anderson's proposal of the resonating valence bond (RVB) state as a fundamental ground state for undoped cuprates [23], chemical substitution in herbertsmithite has been pursued to tune its quantum state. One notable derivative, Y-kapellasite $Y_3Cu_9(OH)_{19}Cl_8$, is an insulating kagome antiferromagnet in which a lattice distortion arises from the displacement of Y atoms, partially releasing the intrinsic frustration [24]. As a result, the magnetic ions $Cu^{2+}(S = 1/2)$ form an original anisotropic kagome lattice, modeled with three distinct nearest-neighbor interactions [25]. Detailed NMR, μSR, and neutron scattering studies [26,27] have established in-plane $(1/3, 1/3)$ magnetic order in a disorder-free single crystal. Further, the magnetic interactions,

*Contact author: dipranjan.chatterjee@physics.ox.ac.uk
†Contact author: P.Puphal@fkf.mpg.de

Published by the American Physical Society under the terms of the Creative Commons Attribution 4.0 International license. Further distribution of this work must maintain attribution to the author(s) and the published article's title, journal citation, and DOI. Open access publication funded by the Max Planck Society.

obtained by spin wave analysis, place the compound in the vicinity of the boundary to a spin liquid phase in the phase diagram computed classically, thus motivating the present high-pressure investigations [26].

Pressure is a powerful nonthermal tuning parameter in quantum materials, capable of altering bandwidth and correlations [28,29], Fermi-surface topology [30–32], magnetism, Kondo physics, and phonon interactions [33–35]. In frustrated magnets, it can be used to separate the roles of disorder and geometric frustration. For example, in pyrochlores, pressure has been shown to induce the coexistence of long-range order and QSL behavior in $Tb_2Ti_2O_7$ [36], drive a transition from QSL to ferromagnetism in $Yb_2Ti_2O_7$ [37], and suppress ferromagnetic correlations in $Tb_2Sn_2O_7$ [38]. Pressure can also reduce disorder, as in the Kitaev candidate material α-$RuCl_3$ [39]. In herbertsmithite, the crystal symmetry and, hence, the perfect kagome lattice are preserved, with only a moderate change of the Cu-O-Cu bond angles, up to 8 GPa until a structural transition occurs [40]. Accordingly, the μSR relaxation and susceptibility remain unchanged under pressure showing that the QSL ground state persists up to at least 3 GPa [40,41]. In contrast, the present Letter examines a kagome antiferromagnet that is both geometrically frustrated and free from site disorder, providing a rare opportunity to isolate and directly probe the role of pure geometric frustration in stabilizing a spin liquid ground state.

$Y_3Cu_9(OH)_{19}Cl_8$, Y-kapellasite features a 1/9 substitution of Cl^- by $(OH)^-$, as compared to $YCu_3(OH)_6Cl_3$ and the shorter Y-OH bonds displace Y atoms out of the kagome plane, distorting the lattice into an anisotropic network with three distinct exchange interactions (Fig. 1). The resulting kagome "skeleton" comprises two inequivalent Cu sites and anisotropic exchange interactions. The structural distortion shortens one Cu1-Cu2 bond to 3.26 Å (green bond), while the remaining Cu-Cu distances remain near 3.38 Å. Concomitantly, the Cu-O-Cu bond angle associated with this shortened bond is reduced to ∼110°, whereas the other angles remain close to $116° - 117°$ [Fig. 3(c)]. The magnetic sublattice can, thus, be viewed as Cu1-Cu1 hexagons (orange) coupled by three distinct interactions: $J_{\hexagon}$ within the hexagons, J along Cu2-Cu1 bonds (blue), and a weaker J' along the shortened Cu1-Cu2 bonds (green). From our previous spin wave analysis [26], we estimated $J_{\hexagon} = J = -140(10)$ K and $J' = -63(7)$ K, consistent with the hierarchy inferred from the bond angles. These interactions yield a Curie-Weiss temperature of $-114(9)$ K, in agreement with independent susceptibility measurements, and place Y-kapellasite in the $(1/3, 1/3)$ antiferromagnetic phase, close to a boundary of a spin liquid regime [25].

Thus, the system exhibits long-range order (LRO) below $T_N = 2.2$ K [26]. Uniaxial strain releases the frustration and strengthens the antiferromagnetic order [27]. On the other hand, disorder can induce a spin liquid state in powders [42]. It is also present in the Br analog [43–45],

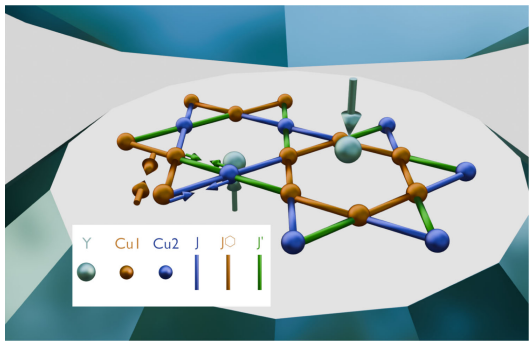


FIG. 1. Schematic view of a single kagome layer of Y-kapellasite inside the diamond anvil cell, highlighting the pressure-tuned magnetic "skeleton" made of two inequivalent Cu sites (Cu1 in orange, Cu2 in blue). The dominant exchange interaction $J_{\hexagon}$ along Cu1-Cu1 bonds (orange), the weaker Cu1-Cu2 interaction J' (green), and the Cu2-Cu1 interaction J (blue) are indicated. Gray arrows illustrate the effect of hydrostatic pressure, which pushes the Y ions (located at the centers of the hexagons) back toward the kagome plane.

where a partial occupancy of the Y site occurs in the kagome plane, thus presenting a mixed system between $YCu_3(OH)_6Cl_3$ (in-plane Y) and $Y_3Cu_9(OH)_{19}Cl_8$ (out of plane Y). In contrast, our single crystals are free from site mixing, maintain a stable Cu^{2+} oxidation state, and possess a well-defined superstructure, resulting in LRO confirmed by NMR, INS, and μSR [26,27] (see Supplemental Material for additional details [46]). Here we study these clean crystals under hydrostatic pressure, using μSR and complementary techniques to investigate how the evolution of the structure enhances the magnetic frustration and drives the nature of the ground state, in stark contrast to chemical pressure resulting in reduced frustration [55] (see Supplemental Materials for more details [46]).

Previous μSR measurements at ambient pressure [26] on single crystal of $Y_3Cu_9(OH)_{19}Cl_8$ revealed a bulk magnetic transition at T_N with a broadly distributed and unusually small (∼8.6 mT) internal field at base temperature. To probe the stability of this ordered state, we performed a pressure-dependent μSR experiment on crushed single crystals in a hydrostatic piston cylinder cell on the GPD spectrometer at the Paul Scherrer Institute. In this setup, a fraction f (50%–70%) of muons stop in the pressure-cell walls, producing a known background relaxation $P_{\text{cell}}(t)$ represented by the dashed line in Fig. 2(a) that can be separated from the sample signal [47].

Figure 2(a) presents the zero-field (ZF) μSR spectra measured at the base temperature $T = 0.28$ K under ambient pressure and applied pressures of 1.14, 1.8, and 2.3 GPa; no hysteresis is observed (see Supplemental Material for more details [46]), as the ambient pressure spectrum is fully recovered after releasing the applied pressure. As expected from previous measurements [26], the ZF spectrum at ambient pressure shows a pronounced dip near 0.4 μs, characteristic of static magnetic order.

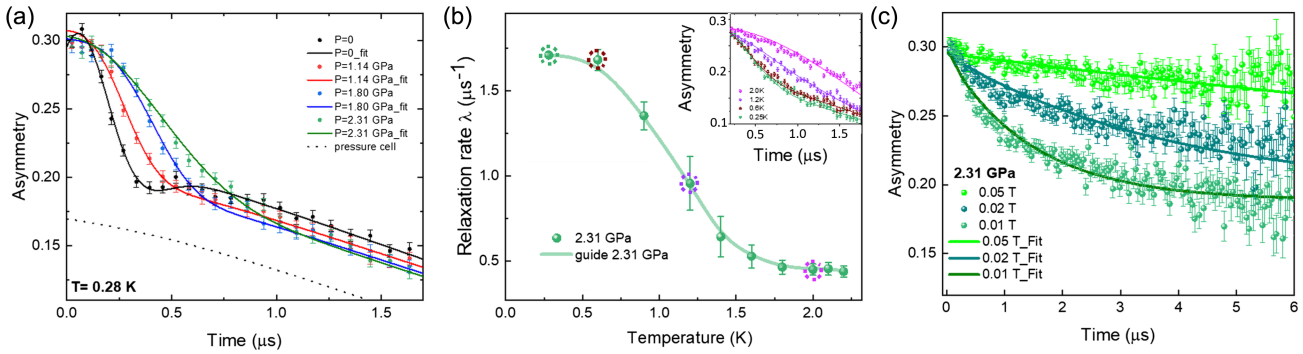


FIG. 2. (a) Zero-field (ZF) asymmetries measured at 0.28 K under different pressures: ambient pressure, 1.14 GPa, 1.8 GPa, and 2.3 GPa. The black dotted line indicates the contribution from the pressure cell. (b) Temperature evolution of the relaxation rate λ at $P = 2.3$ GPa. Inset: zero-field asymmetry spectra measured at 2.0, 1.2, 0.6, and 0.25 K at $P = 2.3$ GPa. (c) Time evolution of LF asymmetries at 0.28 K under three different fields: 0.01 T, 0.02 T, and 0.05 T at 2.3 GPa, along with the corresponding fits to the DKT model [see Eq. (2)] demonstrating a dynamical ground state.

The cell fraction $f = 0.53$ of the signal with the relaxation $P_{\mathrm{cell}}(t)$ was then determined by fitting the ambient pressure sample relaxation as in Ref. [26], with a damped oscillatory term, $\frac{2}{3}\cos(\omega_f t + \phi)e^{-\sigma^2 t^2/2} + (e^{-\lambda_f t}/3)$, where ω_f is the muon precession frequency proportional to the internal field, σ_f the field distribution width, and λ_f the relaxation rate of the 1/3 tail signal. Remarkably, at the maximum applied pressure, the dip disappears, and the asymmetry relaxation is markedly slower, indicating the suppression of static magnetism and the emergence of a dynamical ground state. We further measured the temperature dependence of the ZF asymmetries at $P = 2.3$ GPa, which we could model as

$$a(t) = A_0\left[fP_{\mathrm{cell}}(t) + (1-f)\left(f_r e^{-(\lambda t)^{\alpha}} + (1-f_r)\right)\right], \quad (1)$$

where $A_0 \sim 0.3$ is the initial asymmetry, $f = 0.54(2)$ the cell fraction, and $(1 - f_r) = 0.25$ a minority of weakly relaxing muons [26,42]. For $T \gtrsim 1.6$ K, rapid Cu^{2+} spin fluctuations cause motional narrowing, leaving λ dominated by weak nuclear fields and nearly temperature independent as shown in Fig. 2(b). At lower temperature, $\lambda(T)$ evolves smoothly into a dynamical plateau, as observed for all QSL candidates [7,56,57] and is taken as an indication of the persistent dynamics of correlated spins.

To confirm that the low temperature spin correlations are fully dynamic at 2.3 GPa, we performed an additional longitudinal-field (LF) μSR experiment [Fig. 2(c)]. Fields $H_{LF} > 0.01$ T fully decouple the pressure-cell background [47] and the quasistatic nuclear contribution, leaving only the electronic spin relaxation. If the weak $\lambda = 1.7$ μs^{-1} relaxation observed at low T were of static origin, it should be fully suppressed by fields $\gtrsim 0.02$ T. This is clearly not the case, which demonstrates that the relaxation is of dynamical origin. Accordingly, the LF data shown in Fig. 2(c) were modeled with the standard dynamical Kubo-Toyabe (DKT) function,

$$a_{LF}(t) = (A_0 - A_{bkg})P_{DKT}(t,\nu,\Delta,H_{LF}) + A_{bkg}, \quad (2)$$

where $A_{bkg} \sim A_0 f$, Δ/γ_μ is the width of the distribution of the internal fields and ν their fluctuation rate [58]. Fits of the 0.01, 0.02, and 0.05 T data give $\Delta/\gamma_\mu = 2.9$ mT ($\Delta = 2.41(3)$ MHz) and $\nu = 7.81(2)$ MHz. Since $\nu > \Delta$, the 2.3 GPa state lies deep in the fluctuating regime, with no evidence of spin freezing. The absence of static magnetism despite strong exchange interactions provides direct evidence for a fluctuating, spin-liquid-like, ground state at 2.3 GPa in Y-kapellasite. We note that this ground state differs from the one of powder samples formerly studied in Ref. [42]. Indeed, similar decoupling experiments revealed an inhomogeneous behavior, demonstrating residual disorder in powder samples, at variance with the homogeneous fluctuating ground state induced by pressure in crystals.

To elucidate the pressure-induced dynamical ground state and assess the role of geometric frustration, we investigated the kagome lattice of Y-kapellasite under external pressure using high-pressure single crystal x-ray diffraction (XRD). At ambient pressure, Y-kapellasite crystallizes in the trigonal space group No. 148, $R\bar{3}$, with lattice parameters $a = b = 11.57$ Å and $c = 17.33$ Å. This structure constitutes a supercell and subgroup of $YCu_3(OH)_6Cl_3$ [16]. The zonal (0kl) diffraction maps of the subcell differ markedly from those of the supercell, and remain, independent of pressure as visible in Supplemental Material [46]. Thus, upon application of hydrostatic pressure, the kagome lattice remains isostructural, both at room temperature and at 3 K. However, subtle yet systematic changes in bond lengths and angles modify the magnetic superexchange interactions in an anisotropic fashion. In general, softer bonds are expected to compress more

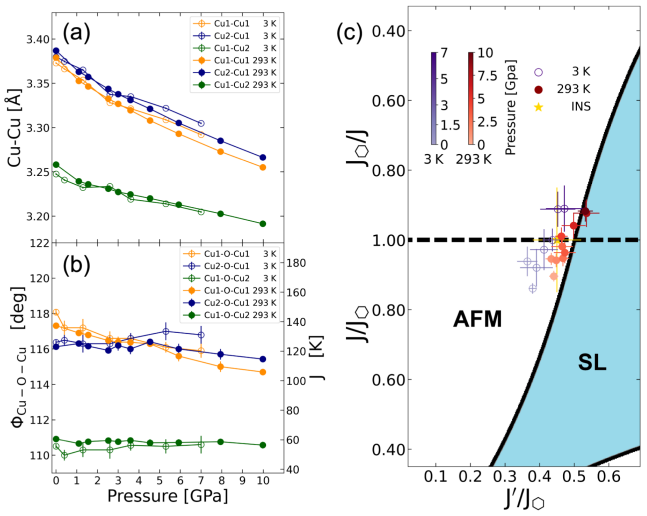


FIG. 3. (a) Pressure dependence of the refined Cu-Cu bond lengths: Cu1-Cu1 (orange), Cu1-Cu2 (green), and Cu2-Cu1 (dark blue). (b) Corresponding pressure evolution of the Cu-O-Cu bond angles defining the superexchange pathways $J_{\bigcirc}$ (Cu1-O-Cu1, orange), J' (Cu1-O-Cu2, green), and J (Cu2-O-Cu1, dark blue). (c) Classical phase diagram of the distorted kagome antiferromagnet as a function of the exchange interactions $J_{\bigcirc}$, J, and J' [25]. The white region denotes the $(1/3, 1/3)$ antiferromagnetic ordered phase, while the blue region corresponds to a spin liquid (SL) regime. The exchange parameters obtained from spin wave analysis of inelastic neutron scattering data are shown as a yellow star [26]. Estimates of the pressure-dependent exchange couplings derived from Eq. (3) are indicated by blue (low temperature) and red (high temperature) symbols, with the applied pressure color coded as indicated in the legend.

strongly, while bonds already under compression remain relatively rigid. Consistent with this expectation, the short Cu1-Cu2 bond (green) exhibits only a weak pressure dependence, whereas the longer Cu1-Cu1 bond (orange) contracts significantly under pressure [Fig. 3(b)]. Similarly, the Cu1-O-Cu1 bond angle decreases substantially, while the Cu1-O-Cu2 angle remains essentially unchanged [Fig. 3(c)]. These trends reflect the pressure-induced relaxation of the Y ions back toward the kagome plane, predominantly affecting the Cu1 sites associated with the dominant interaction $J_{\bigcirc}$.

In cuprate oxides with a single Cu oxidation state, magnetic exchange interactions are governed primarily by superexchange, which depends sensitively on the Cu-O-Cu bond angle φ. In the present case, the exchange can be estimated as

$$J(\mathrm{K}) \approx -1270.5 + 12\varphi, \tag{3}$$

as discussed further in Supplemental Material [46]. Using this empirical relation together with the measured pressure evolution of the bond angles, we trace the trajectory of Y-kapellasite within the magnetic phase diagram [Fig. 3(d)]. Increasing pressure enhances the degree of geometric frustration, driving the system toward the spin liquid regime. While the moderate pressures accessed here (∼2 GPa) do not yet place the material fully inside the spin liquid region inferred from μSR measurements, it is important to note that the phase boundary shown in Fig. 3(d) is based on a classical analysis. Its precise location for a quantum $S = 1/2$ kagome antiferromagnet such as Y-kapellasite remains an open theoretical question.

Pressure tuning provides a natural framework for understanding the emergence of a dynamical state as the anisotropic kagome lattice evolves toward a more isotropic configuration. This highlights the structural integrity of the kagome lattice as a key controlling factor. Y-kapellasite is known to undergo a structural transition near 33 K, clearly manifested in thermal expansion, specific heat, and NMR measurements [26], but not detected by x-ray diffraction, as the Cu-O framework ("skeleton") remains intact and only subtle hydrogen rearrangements occur. Optical spectroscopy, by contrast, is directly sensitive to OH-related phonons. Indeed, Ref. [59] reports the emergence of additional weak modes below 32 K in the spectral range dominated by hydrogen motion, for example, between 3200 and 3500 cm^{-1}.

Motivated by these findings, we measured infrared absorbance spectra under quasihydrostatic pressure, both below and above the transition, in two temperature regimes (14–18 K and 100 K), as shown in Fig. 4. The absence of any abrupt change in the pressure dependence at fixed temperature in either regime indicates that the structural modification is triggered by cooling below 33 K and persists independently of applied pressure, up to at least 10 GPa. Under hydrostatic pressure, we observe both redshifts and blueshifts of phonon modes. Such behavior is expected in a low-symmetry crystal with many unconstrained structural parameters, which need not exhibit a simple correlation with volume changes (see dotted lines in Fig. 4).

Following Ref. [59], we classify the phonon spectra into regions associated with different atomic motions, indicated by black arrows at the bottom of Fig. 4, with their pressure evolution traced by gray dashed lines. Region 2 is dominated by Cu and O vibrations, whereas regions 3 and 4 primarily involve H and O motion. While both redshifts and blueshifts are readily observed in regions 3 and 4, the phonon modes in region 2 exhibit exclusively blueshifts. This reflects the rigidity of the Cu-O bonds forming the structural backbone of the crystal and stabilizing the kagome lattice of Cu^{2+} ions.

In contrast, hydrogen atoms are bonded to a single oxygen and are, therefore, less constrained, consistent with the coexistence of redshifting and blueshifting modes. A representative example is region 4, which contains six calculated phonon modes [59]. These modes begin to separate under pressure already at room temperature.

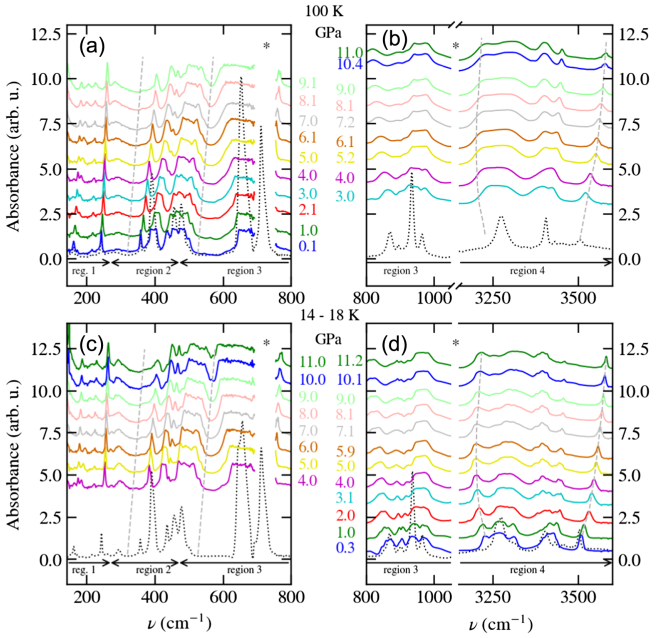


FIG. 4. Low temperature absorbance with increasing pressure at 100 K (a),(b) and at 14-18 K (c),(d). The spectra are shifted along the y axis for clarity. The regions marked by * are excluded because of the contribution from the experimental setup. The dotted line corresponds to the ambient pressure results at 100K and 20K, respectively. Far (1,2) and midinfrared (3,4) regions are indicated by horizontal double arrows separating the regions with the dominant motion of different atoms in the phonon modes. The gray dashed lines are guides for the eyes to highlight the blueshifts and redshifts.

Upon cooling to 14 K, additional modes emerge, which further split and sharpen with increasing pressure. Importantly, applying pressure at low temperature does not induce additional splittings or suppress any phonon modes. In regions 3 and 4, no unresolved hydrogen-related transitions remain. We, thus, conclude that the Cu-O framework remains essentially intact, aside from its continuous pressure-induced evolution observed by x-ray diffraction.

To conclude, we realize the first controlled suppression of magnetic order into a spin-liquid-like, dynamical state, which we investigated by a comprehensive combination of x-ray, optical spectroscopy and μSR measurements under hydrostatic pressure. The pressure-induced fluctuating ground state observed here in crystals should be contrasted with the inhomogeneous spin dynamics observed formerly in powder samples [42], where the spin-liquid-like ground state seems then to be related to some residual, uncontrolled, disorder. Moreover, chemical pressure enhances structural distortions and drives the system away from the SL regime, underscoring external pressure as a uniquely clean and precise tuning parameter. Thus, our Letter establishes Y-kapellasite as an archetypal platform to study the rise and fall of frustrated magnetism in a clean system without disorder. Exploring this material in more detail and performing similar experimental endeavors on other frustrated materials constitutes a major step forward toward the realization of the long sought quantum spin liquid. This Letter paves the way to further experiments under pressure to give evidence for long-range entanglement and fractionalization to characterize the nature of the fluctuating ground state and the possible realization of a quantum spin liquid. Future work can shed light on its relation to the proposed spin liquid in related disordered Br analog compounds at ambient pressure.

Acknowledgments—We acknowledge the ESRF within the in-house proposals No. IH-HC-3746 and No. IH-HC-4021 and SOLEIL for provision of synchrotron radiation. We acknowledge support by the Deutsche Forschungsgemeinschaft (DFG) via No. DR228/68-1 and No. TRR288 (No. 422213477, Project A03). The work of P. D. was funded by the Czech Science Foundation (research Project No. GAČR 23-06810O). A. P. acknowledges support by Hochschuljubiläumsfonds der Stadt Wien (Grant No. H-918729/2022). We acknowledge the support of the French Agence Nationale de la Recherche, under Grant No. ANR-25-CE30-2010-01 "ULTIMAT" and the Fondation Charles Defforey-Institut de France. We thank Jeroen Jacobs for preparation and gas loading of the high-pressure cells, Apostolos Pantousas for single crystal refinement support, and Jens Jakschik for measurement support at the SOLEIL beamtime. D. C. acknowledges funding from UK Research and Innovation (UKRI) through the UK government's Horizon Europe funding guarantee (Grant No. EP/X025861/1) and thanks Prof. Stephen J. Blundell for his support.

Data availability—The XRD datasets can openly be accessed at [60]. The crystallographic structures are available from the joint CCDC/FIZ Karlsruhe database with deposition No. 2467984-2468000. The rest of the data are not publicly available. The data are available from the authors upon reasonable request.

[1] O. A. Starykh, Rep. Prog. Phys. **78**, 052502 (2015); O. A. StarykharXiv:1412.8482.
[2] C. Lacroix, P. Mendels, and F. Mila, *Introduction to Frustrated Magnetism: Materials, Experiments, Theory* (Springer Science & Business Media, New York, 2011), Vol. 164.
[3] L. Balents, Nature (London) **464**, 199 (2010).
[4] Y. Shimizu, K. Miyagawa, K. Kanoda, M. Maesato, and G. Saito, Phys. Rev. Lett. **91**, 107001 (2003).
[5] J. A. M. Paddison, M. Daum, Z. Dun, G. Ehlers, Y. Liu, M. B. Stone, H. Zhou, and M. Mourigal, Nat. Phys. **13**, 117 (2016).
[6] Y. Li, D. Adroja, P. K. Biswas, P. J. Baker, Q. Zhang, J. Liu, A. A. Tsirlin, P. Gegenwart, and Q. Zhang, Phys. Rev. Lett. **117**, 097201 (2016).

[7] P. Mendels, F. Bert, M. A. de Vries, A. Olariu, A. Harrison, F. Duc, J. Trombe, J. Lord, A. Amato, and C. Baines, Phys. Rev. Lett. **98**, 077204 (2007).

[8] T.-H. Han, M. R. Norman, J.-J. Wen, J. A. Rodriguez-Rivera, J. S. Helton, C. Broholm, and Y. S. Lee, Phys. Rev. B **94**, 060409(R) (2016).

[9] J. Wang, W. Yuan, P. M. Singer, R. W. Smaha, W. He, J. Wen, Y. S. Lee, and T. Imai, Nat. Phys. **17**, 1109 (2021).

[10] Z. Feng, W. Yi, K. Zhu, Y. Wei, S. Miao, J. Ma, J. Luo, S. Li, Z. Y. Meng, and Y. Shi, Chin. Phys. Lett. **36**, 017502 (2018).

[11] M. Pinterić, M. Čulo, O. Milat, M. Basletić, B. Korin-Hamzić, E. Tafra, A. Hamzić, T. Ivek, T. Peterseim, K. Miyagawa, K. Kanoda, J. A. Schlueter, M. Dressel, and S. Tomić, Phys. Rev. B **90**, 195139 (2014).

[12] M. Dressel, P. Lazić, A. Pustogow, E. Zhukova, B. Gorshunov, J. A. Schlueter, O. Milat, B. Gumhalter, and S. Tomić, Phys. Rev. B **93**, 081201(R) (2016).

[13] B. Miksch, A. Pustogow, M. J. Rahim, A. A. Bardin, K. Kanoda, J. A. Schlueter, R. Hübner, M. Scheffler, and M. Dressel, Science **372**, 276 (2021).

[14] T. Komatsu, N. Matsukawa, T. Inoue, and G. Saito, J. Phys. Soc. Jpn. **65**, 1340 (1996).

[15] A. Pustogow, Solids **3**, 93 (2022).

[16] R. K. Kremer, S. Bette, J. Nuss, and P. Puphal, Phys. Rev. B **111**, 024424 (2025).

[17] M. M. Bordelon, E. Kenney, C. Liu, T. Hogan, L. Posthuma, M. Kavand, Y. Lyu, M. Sherwin, N. P. Butch, C. Brown, M. J. Graf, L. Balents, and S. D. Wilson, Nat. Phys. **15**, 1058 (2019).

[18] Z. Zhu, P. A. Maksimov, S. R. White, and A. L. Chernyshev, Phys. Rev. Lett. **119**, 157201 (2017).

[19] N. E. Sherman, T. Imai, and Rajiv R. Singh, Phys. Rev. B **94**, 140415(R) (2016).

[20] P. Khuntia, M. Velazquez, Q. Barthélemy, F. Bert, E. Kermarrec, A. Legros, B. Bernu, L. Messio, A. Zorko, and P. Mendels, Nat. Phys. **16**, 469 (2020).

[21] Q. Barthélemy, A. Demuer, C. Marcenat, T. Klein, B. Bernu, L. Messio, M. Velázquez, E. Kermarrec, F. Bert, and P. Mendels, Phys. Rev. X **12**, 011014 (2022).

[22] Q. Barthélemy, E. Lefrançois, J. Baglo, P. Bourgeois-Hope, D. Chatterjee, P. Lefloïc, M. Velázquez, V. Balédent, B. Bernu, N. Doiron-Leyraud, F. Bert, P. Mendels, and L. Taillefer, Phys. Rev. B **107**, 054434 (2023).

[23] P. W. Anderson, Science **235**, 1196 (1987).

[24] P. Puphal, M. Bolte, D. Sheptyakov, A. Pustogow, K. Kliemt, M. Dressel, M. Baenitz, and C. Krellner, J. Mater. Chem. C **5**, 2629 (2017).

[25] M. Hering, F. Ferrari, A. Razpopov, I. I. Mazin, R. Valentí, H. O. Jeschke, and J. Reuther, npj Comput. Mater. **8**, 1 (2022).

[26] D. Chatterjee, P. Puphal, Q. Barthélemy, J. Willwater, S. Süllow, C. Baines, S. Petit, E. Ressouche, J. Ollivier, K. M. Zoch, C. Krellner, M. Parzer, A. Riss, F. Garmroudi, A. Pustogow, P. Mendels, E. Kermarrec, and F. Bert, Phys. Rev. B **107**, 125156 (2023).

[27] J. Wang, M. Spitaler, Y.-S. Su, K. M. Zoch, C. Krellner, P. Puphal, S. E. Brown, and A. Pustogow, Phys. Rev. Lett. **131**, 256501 (2023).

[28] S. Lefebvre, P. Wzietek, S. Brown, C. Bourbonnais, D. Jérome, C. Mézière, M. Fourmigué, and P. Batail, Phys. Rev. Lett. **85**, 5420 (2000).

[29] P. Limelette, P. Wzietek, S. Florens, A. Georges, T. A. Costi, C. Pasquier, D. Jérome, C. Mézière, and P. Batail, Phys. Rev. Lett. **91**, 016401 (2003).

[30] X.-C. Pan, X. Chen, H. Liu, Y. Feng, Z. Wei, Y. Zhou, Z. Chi, L. Pi, F. Yen, F. Song *et al.*, Nat. Commun. **6**, 7805 (2015).

[31] D. Kang, Y. Zhou, W. Yi, C. Yang, J. Guo, Y. Shi, S. Zhang, Z. Wang, C. Zhang, S. Jiang *et al.*, Nat. Commun. **6**, 7804 (2015).

[32] P. Lu, J.-S. Kim, J. Yang, H. Gao, J. Wu, D. Shao, B. Li, D. Zhou, J. Sun, D. Akinwande, D. Xing, and J.-F. Lin, Phys. Rev. B **94**, 224512 (2016).

[33] H. Hegger, C. Petrovic, E. G. Moshopoulou, M. F. Hundley, J. L. Sarrao, Z. Fisk, and J. D. Thompson, Phys. Rev. Lett. **84**, 4986 (2000).

[34] G. Knebel, D. Aoki, J.-P. Brison, and J. Flouquet, J. Phys. Soc. Jpn. **77**, 114704 (2008).

[35] P. Sakrikar, B. Shen, E. H. Poldi, F. Bahrami, X. Hu, E. M. Kenney, Q. Wang, K. W. Fruhling, C. Wang, R. Gupta *et al.*, Nat. Commun. **16**, 4712 (2025).

[36] I. Mirebeau, I. N. Goncharenko, P. Cadavez-Peres, S. T. Bramwell, M. J. P. Gingras, and J. S. Gardner, Nature (London) **420**, 54 (2002).

[37] E. Kermarrec, J. Gaudet, K. Fritsch, R. Khasanov, Z. Guguchia, C. Ritter, K. A. Ross, H. A. Dabkowska, and B. D. Gaulin, Nat. Commun. **8**, 14810 (2017).

[38] I. Mirebeau, I. Goncharenko, H. Cao, and A. Forget, Phys. Rev. B **80**, 220407(R) (2009).

[39] Q. Stahl, T. Ritschel, G. Garbarino, F. Cova, A. Isaeva, T. Doert, and J. Geck, Nat. Commun. **15**, 8142 (2024).

[40] P. Malavi, S. Pal, D. V. S. Muthu, S. Sahoo, S. Karmakar, and A. K. Sood, Phys. Rev. B **101**, 214402 (2020).

[41] Q. Barthélemy, Thesis, Université Paris-Saclay, Francais, 2020.

[42] Q. Barthélemy, P. Puphal, K. M. Zoch, C. Krellner, H. Luetkens, C. Baines, D. Sheptyakov, E. Kermarrec, P. Mendels, and F. Bert, Phys. Rev. Mater. **3**, 074401 (2019).

[43] Z. Zeng, X. Ma, S. Wu, H.-F. Li, Z. Tao, X. Lu, X. H. Chen, J.-X. Mi, S.-J. Song, G.-H. Cao, G. Che, K. Li, G. Li, H. Luo, Z. Y. Meng, and S. Li, Phys. Rev. B **105**, L121109 (2022).

[44] J. Liu, L. Yuan, X. Li, B. Li, K. Zhao, H. Liao, and Y. Li, Phys. Rev. B **105**, 024418 (2022).

[45] Z. Zeng, C. Zhou, H. Zhou, L. Han, R. Chi, K. Li, M. Kofu, K. Nakajima, Y. Wei, W. Zhang, D. G. Mazzone, Z. Y. Meng, and S. Li, Nat. Phys. **20**, 1097 (2024).

[46] See Supplemental Material at http://link.aps.org/supplemental/10.1103/3pmg-b78n for further details, which includes Refs. [47–54], for additional information.

[47] R. Khasanov, Z. Guguchia, A. Maisuradze, D. Andreica, M. Elender, A. Raselli, Z. Shermadini, T. Goko, F. Knecht, E. Morenzoni *et al.*, High Press. Res. **36**, 140 (2016).

[48] R. Khasanov, J. Appl. Phys. **132**, 190903 (2022).

[49] M. Mezouar, G. Garbarino, S. Bauchau, W. Morgenroth, K. Martel, S. Petitdemange, P. Got, C. Clavel, A. Moyne, H.-P. Van Der Kleij *et al.*, High Press. Res. **44**, 1 (2024).

[50] G. Garbarino, M. E. Hanfland, S. Gallego-Parra, A. D. Rosa, M. Mezouar, D. Duran, K. Martel, E. Papillon, T. Roth, P. Got *et al.*, High Press. Res. **44**, 199 (2024).
[51] D. Boldrin, B. Fåk, M. Enderle, S. Bieri, J. Ollivier, S. Rols, P. Manuel, and A. S. Wills, Phys. Rev. B **91**, 220408 (2015).
[52] E. Kermarrec, A. Zorko, F. Bert, R. H. Colman, B. Koteswararao, F. Bouquet, P. Bonville, A. Hillier, A. Amato, J. van Tol, A. Ozarowski, A. S. Wills, and P. Mendels, Phys. Rev. B **90**, 205103 (2014).
[53] A. Celeste, F. Borondics, and F. Capitani, High Press. Res. **39**, 608 (2019).
[54] E. Grüneisen, Ann. Phys. (Berlin) **344**, 257 (1912).
[55] J. A. Krieger, T. J. Hicken, H. Luetkens, R. K. Kremer, and P. Puphal, Phys. Rev. Res. **7**, 033021 (2025).
[56] J. Orain, L. Clark, F. Bert, P. Mendels, P. Attfield, F. Aidoudi, R. E. Morris, P. Lightfoot, A. Amato, and C. Baines, J. Phys. Conf. Ser. **551**, 012004 (2014).
[57] B. Fåk, E. Kermarrec, L. Messio, B. Bernu, C. Lhuillier, F. Bert, P. Mendels, B. Koteswararao, F. Bouquet, J. Ollivier *et al.*, Phys. Rev. Lett. **109**, 037208 (2012).
[58] R. S. Hayano, Y. J. Uemura, J. Imazato, N. Nishida, T. Yamazaki, and R. Hubo, Phys. Rev. B **20**, 850 (1979).
[59] P. Doležal, T. Biesner, Y. Li, R. Mathew Roy, S. Roh, R. Valentí, M. Dressel, P. Puphal, and A. Pustogow, Phys. Rev. B **110**, 174445 (2024).
[60] B. Wehinger, F. Abbruciati, P. Puphal, T. Biesner, G. Garbarino, and J. E. F. S. Rodrigues, European Synchrotron Radiation Facility, 2025, 10.15151/ESRF-DC-2191835598.